blood®
Brief Report

RED CELLS, IRON, AND ERYTHROPOIESIS

Modulation of the HIF2α-NCOA4 axis in enterocytes attenuates iron loading in a mouse model of hemochromatosis

Nupur K. Das,[1] Chesta Jain,[1] Amanda Sankar,[1] Andrew J. Schwartz,[1] Naiara Santana-Codina,[2] Sumeet Solanki,[1] Zhiguo Zhang,[1] Xiaoya Ma,[1] Sanjana Parimi,[1] Liangyou Rui,[1] Joseph D. Mancias,[2] and Yatrik M. Shah[1,3]

[1]Department of Molecular and Integrative Physiology, University of Michigan, Ann Arbor, MI; [2]Division of Radiation and Genome Stability, Department of Radiation Oncology, Dana-Farber Cancer Institute, Boston, MA; and [3]Department of Internal Medicine, Division of Gastroenterology, University of Michigan, Ann Arbor, MI

KEY POINTS

- **Mouse models show that iron homeostasis in hemochromatosis, but not in anemia, is integrated into ferritinophagy.**
- **Disrupting intestinal ferritinophagy protects mice from iron overload, but does not alter iron deficiency.**

Intestinal iron absorption is activated during increased systemic demand for iron. The best-studied example is iron deficiency anemia, which increases intestinal iron absorption. Interestingly, the intestinal response to anemia is very similar to that of iron overload disorders, as both the conditions activate a transcriptional program that leads to a hyperabsorption of iron via the transcription factor hypoxia-inducible factor 2α (HIF2α). However, pathways for selective targeting of intestine-mediated iron overload remain unknown. Nuclear receptor coactivator 4 (NCOA4) is a critical cargo receptor for autophagic breakdown of ferritin and the subsequent release of iron, in a process termed ferritinophagy. Our work demonstrates that NCOA4-mediated intestinal ferritinophagy is integrated into systemic iron demand via HIF2α. To demonstrate the importance of the intestinal HIF2α/ferritinophagy axis in systemic iron homeostasis, whole-body and intestine-specific NCOA4$^{-/-}$ mouse lines were generated and assessed. The analyses revealed that the intestinal and systemic response to iron deficiency was not altered after disruption of intestinal NCOA4. However, in a mouse model of hemochromatosis, ablation of intestinal NCOA4 was protective against iron overload. Therefore, NCOA4 can be selectively targeted for the management of iron overload disorders without disrupting the physiological processes involved in the response to systemic iron deficiency.

Introduction

Intestinal iron absorption is regulated by hypoxia inducible factor-2α (HIF2α).[1] Intestinal HIF2α signaling is integrated into systemic cues for iron requirements via the hepatic hormone hepcidin and the iron exporter ferroportin (Fpn1).[2] During increased systemic iron requirements, iron is released from ferritin (FTN)[3] by ferritinophagy via lysosomal degradation mediated by nuclear receptor coactivator 4 (NCOA4).[4,5] Ferritinophagy is also regulated by intracellular iron.[6] The significance of intestinal iron handling in systemic demand and erythropoiesis and the role of intestinal FTN in iron absorption are well known.[7,8] However, questions remain regarding how ferritinophagy is integrated into systemic iron regulation. In this work, using genetic mouse models of HIF2α and NCOA4 perturbation, we showed that the intestinal HIF2α/ferritinophagic axis is essential for systemic iron regulation, and intestinal NCOA4 can be therapeutically targeted to treat iron overload disorders.

Study design

Animals and treatments

Whole-body NCOA4-knockout (KO) (NCOA4$^{\Delta WB}$) mice and intestine-specific lines HIF-2αKO: HIF2α$^{\Delta IE}$, VhlKO: Vhl$^{\Delta IE}$, and Vhl-HIF2αKO: Vhl/HIF2α$^{\Delta IE}$; and tamoxifen-inducible, liver-specific hepcidin KO mice (HAMP$^{\Delta Liv}$: Alb^{CreERT2}; HAMP$^{fl/fl}$) have been described.[2,9] The intestine-specific NCOA4-KO (NCOA4$^{\Delta IE}$) line was generated by crossing NCOA4$^{F/F10}$ with villin-Cre mice of the C57BL/6J background. For baseline studies, a standard diet (iron, 240 ppm; 5001; Laboratory Diet), and for iron studies, an iron-enriched diet (350 ppm; 115180), or low-iron (<5 ppm; 115072) diet (Dyets Inc) were used. Phenylhydrazine (Phz)-induced hemolysis (intraperitoneal injections; 60 mg/kg body weight on 2 consecutive days), followed by euthanasia within 0, 3, or 6 days of the second injection and oral administration of FG-4592 (12.5 mg/kg per day, 5 days; Cayman Chemicals). Mucosal scrapings to isolate enterocytes were used in all experiments.

CRISPR-mediated hepcidin-KO model

Two guide RNAs targeting mouse hepcidin (supplemental Table 1) were cloned in a CRISPR-Cas9–containing adenovirus dual gRNA expression vector (pAV[CRISPR]-hCAS9; VectorBuilder, Inc) (supplemental Figure 5A). The adenovirus (AV) injection contained 3×10^{11} particles per animal via tail vein (supplemental Figure 5B).

Antibodies

NCOA4 antibodies included anti-rabbit A302-272A (30968; Bethyl Laboratories [BL]); anti-goat (1:200, sc-30968; Santa Cruz Biotechnology); anti-rabbit ferritin H (Cell Signaling Technology [CST]; 2998); anti-rabbit HIF-2α (BL; A700-003); anti-rabbit IRP2 (CST; 37135); anti-rabbit DMT1 (Alpha Diagnostic International [ADI]; NRAMP21-A); anti-rabbit ferroportin 1(ADI; MTP11-A); anti-mouse actin, (60008-1-Ig; 1:10 000; Proteintech;); anti-rabbit LAMP1 (sc-20011; Santa Cruz Biotechnology); and anti-rabbit LAMP2 (7125116; Invitrogen). Dilutions were 1:1000, unless otherwise specified.

Immunohistochemistry

Swiss-rolled, frozen, 7-μm sections fixed in 4% paraformaldehyde in phosphate-buffered saline and incubated overnight at 4°C with rabbit anti-NCOA4 antibody (1:100; BL), were incubated for 1 hour at room temperature with Alexa Fluor 488–labeled goat anti-rabbit IgG (1:500; Molecular Probes, Inc).

Luciferase assay

A 1-kb (relative to the transcription start site) mouse NCOA4 promoter region was cloned in pGL3 basic vector between *Nhe*I and *Xho*I (Promega). HIF1α, HIF2α overexpressing plasmids, and the luciferase assay have been described.[9]

Serum analysis

Iron and transferrin saturation (K392; Biovision), alanine aminotransferase and aspartate aminotransferase (MAK052 and MAK055, respectively; Sigma Aldrich), and erythropoietin (EPO; MEP00B; R&D Systems).

Hematology, iron staining, quantitative reverse transcription-polymerase chain reaction[11]; human intestinal organoid generation[12]; enterocyte membrane[13] and lysosome isolation[14]; chromatin immunoprecipitation assay[1]; and iron quantification by inductively coupled plasma mass spectrometry[15] have been described.

Primers

The PCR primers are listed in supplemental Table 1.

Statistics

Results are expressed as the mean ± standard error of the mean. The significance between 2 groups was determined by a 2-tailed, unpaired Student's *t* test. Significance among multiple groups was calculated by 1-way analysis of variance followed by Tukey's post hoc test or by 2-way analysis of variance followed by Sidak's multiple-comparison test. GraphPad Prism 8.0 was used for statistical analyses.

Results and discussion

Intestinal NCOA4 is a novel HIF2α target gene

NCOA4 is highly expressed in the small intestine (Figure 1A). Duodenal NCOA4 RNA and protein expression are induced in dietary iron deficiency and Phz-mediated hemolytic anemia (Figure 1B-C; supplemental Figure 1A-E). Single-cell transcriptomic analysis has revealed that NCOA4 expression is more abundantly expressed in differentiated enterocytes than in other intestinal epithelial or stem cell lineages.[16,17] NCOA4 (Figure 1D) and divalent metal transporter 1 (DMT1) RNA expression is significantly upregulated in differentiated human intestinal organoids by iron chelator deferoxamine or hypoxia (1% O_2; supplemental Figure 1F). The induction observed in NCOA4 and DMT1 RNA and NCOA4 protein levels during iron deficiency were abolished in the intestine-specific HIF2α-KO ($HIF2\alpha^{\Delta IE}$) mouse duodenum (Figure 1E-G). Furthermore, duodenal NCOA4 RNA and protein expressions were induced in pharmacological (FG4592, a PHD inhibitor) and genetic (intestine-specific HIF overexpression [$Vhl^{\Delta IE}$]) models of HIF activation (Figure 1G-I). A robust increase in FTN heavy chain (FTN H) expression in the $Vhl^{\Delta IE}$ duodenum (Figure 1I) is suggestive of an increase in HIF2α-dependent iron absorption and a corresponding downregulation of iron regulatory protein 2 (IRP2) is indicative of an active iron response element-IRP feedback system (Figure 1I). Increased lysosomal FTN in the $Vhl^{\Delta IE}$ duodenum indicates that NCOA4-mediated lysosomal FTN enrichment is HIF dependent (Figure 1J). Indeed, duodenal NCOA4 and DMT1 induction is completely abolished in the intestine-specific Vhl-HIF2α double-KO mice (Figure 1K-L; supplemental 1H). Subsequent promoter activity analysis of the human intestinal cell lines HCT116 and Caco-2 demonstrated that intestinal NCOA4 was selectively HIF2α dependent (Figure 1M). An NCOA4 promoter analysis revealed the presence of a canonical hypoxia response element (supplemental Figure 1I) and chromatin immunoprecipitation assay of the $Vhl^{\Delta IE}$ duodenum confirmed the binding of HIF2α at the NCOA4 promoter (Figure 1N).

Intestinal NCOA4 is expendable in iron deficiency but is essential in iron overload

In agreement with previous reports, whole-body NCOA4-KO ($NCOA4^{\Delta WB}$) mice (generated by CRISPR/CAS9; supplemental Figures 2A-E and 3A-B) basally exhibited hypochromia with microcytosis (normal hemoglobin, low mean corpuscular height [MCH], and low mean corpuscular volume [MCV]) (supplemental Figure 3C).[6,10] Interestingly, no changes were observed in hepatic hepcidin. Lower renal erythropoietin (EPO) RNA expression (supplemental Figure 3D), but unaltered serum EPO (supplemental Figure 3E) were also noted. Phz-treated $NCOA4^{\Delta WB}$ mice exhibited higher tissue FTN H expression (supplemental Figure 4A). $NCOA4^{\Delta WB}$ mice exhibited lowered hemoglobin and hematocrit after Phz treatment, suggesting a possible role of ferritinophagy in acute iron demand (supplemental Figure 4B). Phz-treated $NCOA4^{\Delta WB}$ mice had significantly higher serum EPO on day 3, but no difference on day 6 (supplemental Figure 4C), reflected in the improved MCV and MCH values (supplemental Figure 4B). In the $NCOA4^{\Delta WB}$ mice receiving an iron-deficient diet (1 week), liver and splenic FTN H expression was significantly higher than in the $NCOA4^{F/F}$ cohort (supplemental Figure 5A). Intriguingly, FTN was significantly reduced in both $NCOA4^{F/F}$ and $NCOA4^{\Delta WB}$ duodenum during dietary iron deficiency (supplemental Figure 5A). This result suggests an active

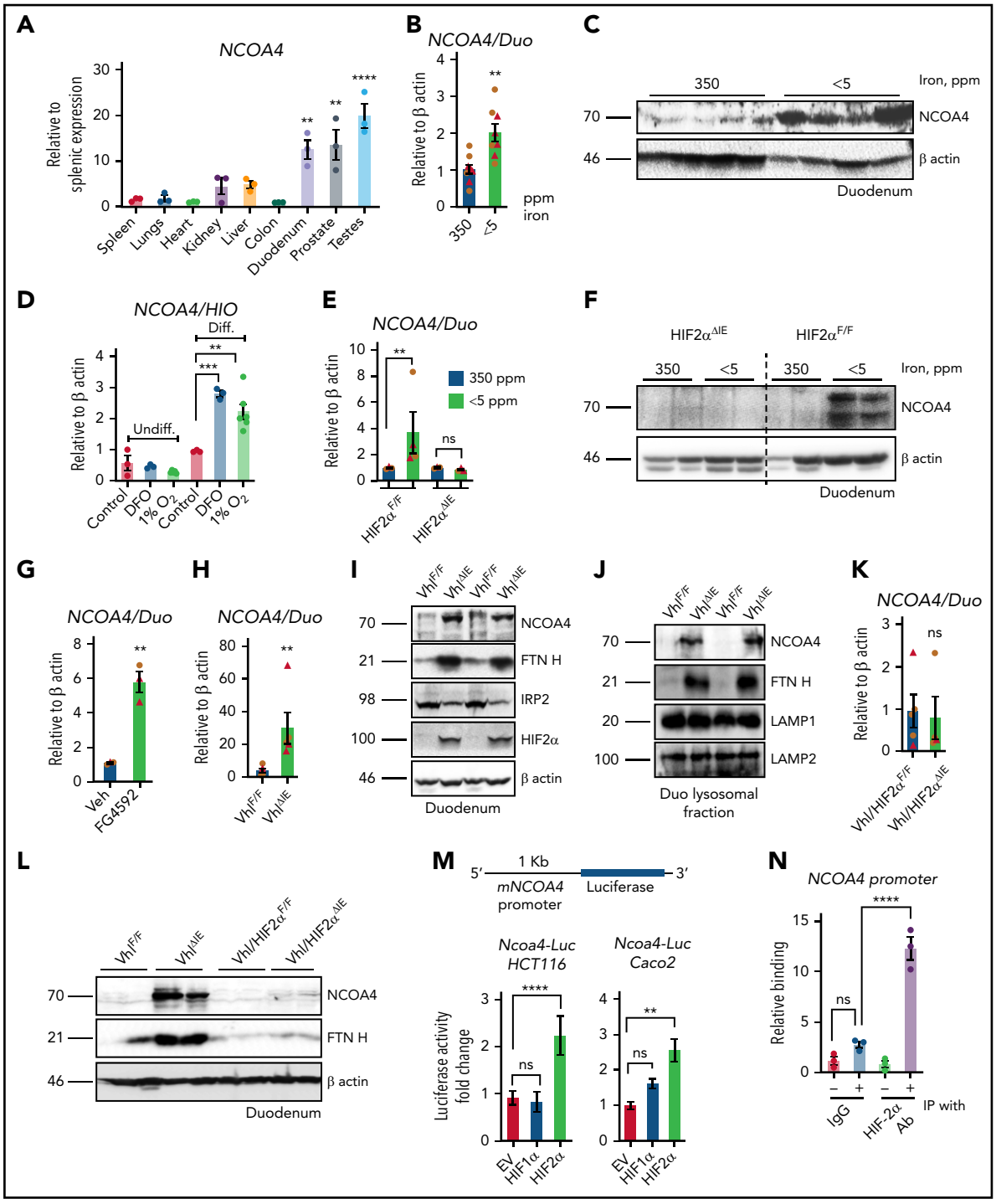

Figure 1. Intestinal NCOA4 is a HIF2α target gene. (A) NCOA4 gene expression analysis by quantitative polymerase chain reaction (qPCR) in mouse tissues; data were normalized to β-actin values, followed by fold change comparison with splenic NCOA4 expression. Wild-type mice were treated with 350- or <5-ppm iron diets for 2 weeks, followed by duodenal NCOA4 gene expression (B) and western blot analysis (C). (D) NCOA4 gene expression analysis in undifferentiated (Undiff.) and differentiated (Diff.) human intestinal organoids treated with deferoxamine (DFO), 100 μM or 1% O_2 for 16 hours. Wild-type ($HIF2\alpha^{F/F}$) and intestine-specific HIF2α ($HIF2\alpha^{\Delta IE}$) KO mice were treated with 350- or <5-ppm iron diets for 2 weeks, followed by duodenal NCOA4 gene expression (E) and western analysis (F). Duodenal NCOA4 gene expression in vehicle (phosphate-buffered saline) or FG4592-treated mice (G), and wild-type ($Vhl^{F/F}$) or intestine-specific Vhl KO ($Vhl^{\Delta IE}$) mice (H). (I) Duodenal NCOA4, FTN H, IRP2, and HIF2α western blot analysis in $Vhl^{F/F}$ and $Vhl^{\Delta IE}$ mice. (J) Duodenal NCOA4 and FTN H western analysis in lysosomal fraction. Duodenal NCOA4 gene expression analysis (K), and duodenal NCOA4 and FTN H western analysis (L) in wild-type ($Vhl/HIF2\alpha^{F/F}$) and intestine-specific Vhl-HIF2α double-KO ($Vhl/HIF2\alpha^{\Delta IE}$) mice. (M) NCOA4 promoter analysis by luciferase assay in HCT116 and Caco-2 cells cotransfected with empty vector (EV), HIF-1α, or HIF-2α. (N) Chromatin immunoprecipitation (IP) assay in the $Vhl^{\Delta IE}$ duodenal epithelial cells relative to normal anti-rabbit IgG. Mice were 4 to 6 weeks old. Female (brown circles); male (red triangles). All data are mean ± standard error of the mean. *$P < .05$; **$P < .01$; ***$P < .001$; ****$P < .0001$.

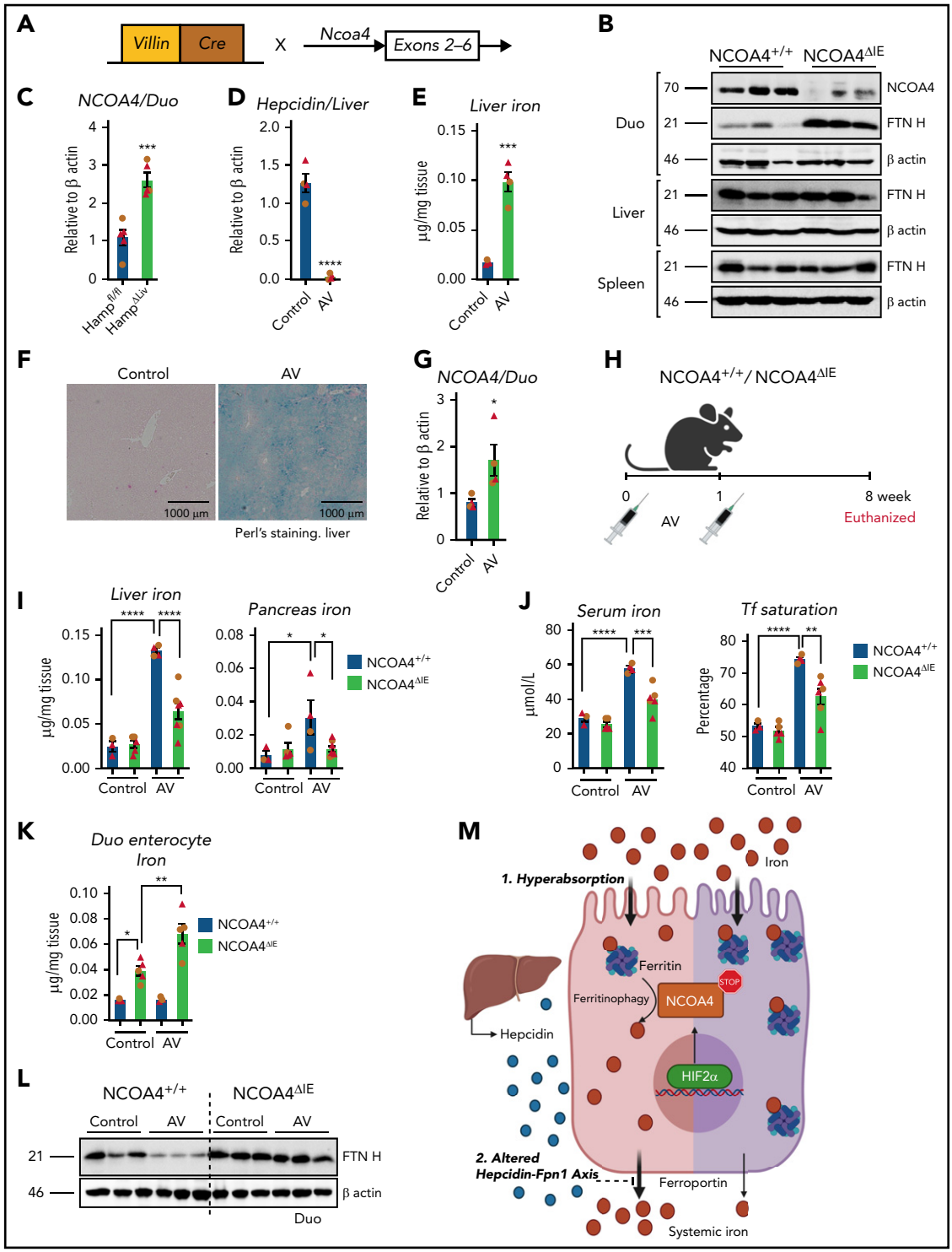

Figure 2. Intestine-specific NCOA4 KO mice are protected from systemic iron overload. (A) Schematic depicting the generation of the intestine-specific NCOA4KO ($NCOA4^{\Delta IE}$) mouse line. (B) Western analysis in the wild-type and $NCOA4^{\Delta IE}$ mice in the duodenum, liver, and spleen. (C) Duodenal NCOA4 gene expression analysis in wild-type vs $NCOA4^{\Delta Liv}$ mice. Characterization of mice treated with vehicle or AV (adenovirus harboring CRISP R-hepcidin guide RNA construct) by assessment for hepatic hepcidin gene expression (D), tissue iron quantification (E), Perl's Prussian blue staining (F), and duodenal NCOA4 gene expression (G). (H) Schematic of AV treatment in $NCOA4^{\Delta IE}$ and wild-type littermates. Hepatic and pancreatic iron (I), serum iron and transferrin (Tf) saturation (J), duodenal enterocyte iron (K), and duodenal FTN H western analyses (L) in the $NCOA4^{\Delta IE}$ and wild-type mice after AV-induced disruption of hepcidin. (M) Schematic of HIF2α/NCOA4 ferritinophagy axis in conditions of intestinal iron hyperabsorption and altered hepcidin-Fpn1 axis, showing active NCOA4-mediated ferritin breakdown facilitates systemic iron loading (left, pink) and how intestine-specific silencing of NCOA4 attenuates it (right, purple). Mice were 4 to 6 weeks of age. Female, brown circles; male, red triangles. All data are mean ± standard error of the mean. $^*P < .05$; $^{**}P < .01$; $P < .001$; $P < .0001$.

IRP-mediated FTN translational inhibition in iron-deficient enterocytes, and/or NCOA4 independent FTN turnover via bulk- or ATG5-dependent autophagy. NCOA4$^{\Delta WB}$ mice on normal (350-ppm) iron diet basally show microcytosis (low MCV) and hypochromia (low MCH), but NCOA4$^{\Delta WB}$ mice on iron-deficient diet did not show further alterations (supplemental Figure 5B). Tissue FTN H and FTN light chain (FTN L) RNA expression analyses did not show a significant difference among all groups of the experiment (supplemental Figure 5C).

To determine the role of intestinal ferritinophagy in systemic iron metabolism, intestine-specific NCOA4-KO (NCOA4$^{\Delta IE}$) mice were generated (Figure 2A). NCOA4$^{\Delta IE}$ duodenum showed increased FTN H expression (Figure 2B), but unaltered hematology compared with NCOA4$^{F/F}$ mice (supplemental Figure 6A). Phz-treated NCOA4$^{\Delta IE}$ mice did not show major hematological changes except a significant increase in MCV (supplemental Figure 6B), and no changes in hepatic hepcidin RNA expression, both basally and after Phz treatment was observed (supplemental Figure 6C). NCOA4$^{\Delta IE}$ mice revealed significant intestinal iron retention (supplemental Figure 6D), suggesting the possible role of NCOA4 in intestinal iron mobilization. However, disruption of intestinal NCOA4 did not alter systemic iron homeostasis in basal or anemic conditions. The intestinal response to increased systemic iron demand was similar during both deficiency and overload (primary and secondary). Intestinal HIF2α was activated, and intestinal iron absorption was increased.[1,2,11,13,18] Consistent with this, a genetic iron overload model (hepatic hepcidin disruption (HAMP$^{\Delta Liv}$) demonstrated a significant increase in intestinal NCOA4 (Figure 2C).[2] To understand genetically whether intestinal ferritinophagy alters iron overload, we would have to cross the NCOA4$^{\Delta IE}$ and HAMP$^{\Delta Liv}$ mice, with possible confounding intestinal and hepatic disruption of both NCOA4 and hepcidin. Therefore, we generated an AV-mediated CRISPR/CAS9-based hepcidin KO mouse model, an efficient gene-silencing approach with broad tropism[19] (Figure 2D-F; supplemental Figure 7A-B). In agreement with Figure 2C, duodenal NCOA4 mRNA expression was increased after hepcidin disruption by AV (Figure 2G). NCOA4$^{\Delta IE}$ or littermate controls were treated with control or CRISPR/CAS9-based hepcidin KO AV (Figure 2H). After 8 weeks, hepatic hepcidin RNA expression was equally suppressed in both AV-treated groups (supplemental Figure 7C). The induction observed in the hepatic FTN H protein levels of the AV-treated NCOA4$^{F/F}$ mice was completely abolished in the corresponding NCOA4$^{\Delta IE}$ cohort (supplemental Figure 7D). Furthermore, assessment of liver, pancreas, serum iron, and transferrin saturation revealed that NCOA4$^{\Delta IE}$ mice are significantly protected from developing iron overload (Figure 2I-J). Hepcidin KO in NCOA4$^{\Delta IE}$ mice exhibited increased intestinal iron retention as evidenced by duodenal enterocyte iron and FTN protein expression analyses (Figure 2K-L). However, duodenal DMT1 and Fpn1 proteins were increased similarly after hepcidin disruption in NCOA4$^{F/F}$ or NCOA4$^{\Delta IE}$ mice (supplemental Figure 7E). Serum transaminase levels (alanine aminotransferase and aspartate aminotransferase) were not altered, suggesting that iron overload–mediated hepatic damage has yet to set in (supplemental Figure 7F). These data suggest that hyperabsorption of iron can be attenuated by inhibition of intestinal NCOA4.

Our work suggests that enterocyte iron and FTN levels are critical determinants of the necessity for NCOA4 in intestinal iron absorption. In hemochromatosis, relative to iron deficiency, the increased iron flux led to high FTN turnover and enhanced requirement of ferritinophagy in intestinal iron absorption (Figure 2M). Therefore, genetic and pharmacological approaches to specifically target intestinal NCOA4 may be beneficial for managing iron overload disorders. Targeting intestine-specific ferritinophagy by bulk autophagy inhibitors[20] or intestine targeting of NCOA4 via gene-silencing methods[21] carries enormous therapeutic potential, either as a single agent or combination therapy with other investigational agents such as DMT1 inhibitors or DMT1/transmembrane protease serine 6 antisense oligonucleotides.

Acknowledgments

The visual abstract and schematic diagram (Figure 2M) were created with BioRender.com.

This work was supported by National Institutes of Health, National Cancer Institute grants R01CA148828 and R01CA245546; National Institute of Diabetes and Digestive and Kidney Diseases (NIDDK) grants R01DK095201 (Y.M.S.) and R01DK124384 (J.D.M.); a Burroughs Wellcome Fund Career Award for Medical Scientists (J.D.M.); and the University of Michigan Comprehensive Cancer Center (UMCCC) Core Grant P30CA046592, the University of Michigan GI SPORE Molecular Pathology and Biosample Core (P50CA130810), and the Center for Gastrointestinal Research (DK034933).

Authorship

Contribution: N.K.D. and Y.M.S. conceived and designed the study; N.K.D., C.J., A.S., A.J.S., N.S.-C., S.S., Z.Z., X.M., and S.P. developed the methodologies; N.K.D., C.J., A.S., A.J.S., N.S.-C., S.S., Z.Z., X.M., and S.P. acquired the data; N.K.D., C.J., L.R., J.D.M., and Y.M.S. analyzed and interpreted the data; J.D.M. provided the key reagents; N.K.D. and Y.M.S. supervised the study and wrote the manuscript; and all authors edited and provided inputs to the manuscript.

Conflict-of-interest disclosure: J.D.M. holds a patent pertaining to the autophagic control of iron metabolism. The remaining authors declare no competing financial interests.

ORCID profiles: N.K.D., 0000-0002-5652-1134; Z.Z., 0000-0002-0331-7682; L.R., 0000-0001-8433-8137; Y.M.S., 0000-0002-2487-4816.

Correspondence: Yatrik M. Shah, Department of Molecular and Integrative Physiology, University of Michigan, 1301 East Catherine St, Ann Arbor, MI 48109; e-mail: shahy@umich.edu.

Footnotes

Submitted 23 July 2021; accepted 22 December 2021; prepublished online on *Blood* First Edition 6 January 2022; DOI 10.1182/blood.2021013452.

All reagent, protocols, and mouse models will be shared in response to e-mail request to the corresponding author.

The online version of this article contains a data supplement.

There is a *Blood* Commentary on this article in this issue.

The publication costs of this article were defrayed in part by page charge payment. Therefore, and solely to indicate this fact, this article is hereby marked "advertisement" in accordance with 18 USC section 1734.

REFERENCES

1. Shah YM, Matsubara T, Ito S, Yim SH, Gonzalez FJ. Intestinal hypoxia-inducible transcription factors are essential for iron absorption following iron deficiency. *Cell Metab*. 2009;9(2):152-164.
2. Schwartz AJ, Das NK, Ramakrishnan SK, et al. Hepatic hepcidin/intestinal HIF-2α axis maintains iron absorption during iron deficiency and overload. *J Clin Invest*. 2019; 129(1):336-348.
3. Arosio P, Ingrassia R, Cavadini P. Ferritins: a family of molecules for iron storage, antioxidation and more. *Biochim Biophys Acta*. 2009;1790(7):589-599.
4. Mancias JD, Wang X, Gygi SP, Harper JW, Kimmelman AC. Quantitative proteomics identifies NCOA4 as the cargo receptor mediating ferritinophagy. *Nature*. 2014; 509(7498):105-109.
5. Dowdle WE, Nyfeler B, Nagel J, et al. Selective VPS34 inhibitor blocks autophagy and uncovers a role for NCOA4 in ferritin degradation and iron homeostasis in vivo. *Nat Cell Biol*. 2014;16(11):1069-1079.
6. Bellelli R, Federico G, Matte' A, et al. NCOA4 deficiency impairs systemic iron homeostasis. *Cell Rep*. 2016;14(3):411-421.
7. Shah YM, Xie L. Hypoxia-inducible factors link iron homeostasis and erythropoiesis. *Gastroenterology*. 2014;146(3):630-642.
8. Vanoaica L, Darshan D, Richman L, Schümann K, Kühn LC. Intestinal ferritin H is required for an accurate control of iron absorption. *Cell Metab*. 2010;12(3):273-282.
9. Das NK, Schwartz AJ, Barthel G, et al. Microbial metabolite signaling is required for systemic iron homeostasis. *Cell Metab*. 2020;31(1):115-130.e6.
10. Santana-Codina N, Gableske S, Quiles del Rey M, et al. NCOA4 maintains murine erythropoiesis via cell autonomous and non-autonomous mechanisms. *Haematologica*. 2019;104(7):1342-1354.
11. Anderson ER, Taylor M, Xue X, et al. Intestinal HIF2α promotes tissue-iron accumulation in disorders of iron overload with anemia. *Proc Natl Acad Sci USA*. 2013; 110(50):E4922-E4930.
12. Finkbeiner SR, Freeman JJ, Wieck MM, et al. Generation of tissue-engineered small intestine using embryonic stem cell-derived human intestinal organoids. *Biol Open*. 2015;4(11):1462-1472.
13. Taylor M, Qu A, Anderson ER, et al. Hypoxia-inducible factor-2α mediates the adaptive increase of intestinal ferroportin during iron deficiency in mice. *Gastroenterology*. 2011;140(7):2044-2055.
14. Graham JM. Isolation of lysosomes from tissues and cells by differential and density gradient centrifugation. *Curr Protoc Cell Biol*. 2001;chapter 3:unit 3.6.
15. Choi EK, Aring L, Das NK, et al. Impact of dietary manganese on experimental colitis in mice. *FASEB J*. 2020;34(2):2929-2943.
16. Elmentaite R, Ross ADB, Roberts K, et al. Single-cell sequencing of developing human gut reveals transcriptional links to childhood Crohn's disease. *Dev Cell*. 2020;55(6):771-783.e5.
17. Wang Y, Song W, Wang J, et al. Single-cell transcriptome analysis reveals differential nutrient absorption functions in human intestine. *J Exp Med*. 2020;217(2): e20191130.
18. Das N, Xie L, Ramakrishnan SK, Campbell A, Rivella S, Shah YM. Intestine-specific disruption of hypoxia-inducible factor (HIF)-2α improves anemia in sickle cell disease. *J Biol Chem*. 2015;290(39):23523-23527.
19. Wang D, Mou H, Li S, et al. Adenovirus-mediated somatic genome editing of Pten by CRISPR/Cas9 in mouse liver in spite of Cas9-specific immune responses. *Hum Gene Ther*. 2015;26(7):432-442.
20. Mauthe M, Orhon I, Rocchi C, et al. Chloroquine inhibits autophagic flux by decreasing autophagosome-lysosome fusion. *Autophagy*. 2018;14(8):1435-1455.
21. Ball RL, Bajaj P, Whitehead KA. Oral delivery of siRNA lipid nanoparticles: fate in the GI tract. *Sci Rep*. 2018;8(1):2178.